Acoustic focussing for sedimentation-free high-throughput imaging of microalgae

Björn Hammarström [2] · Massimo Vassalli [3] · Peter Glynne-Jones [1]

Abstract

Microalgae play a key role in aquatic ecology, and methods providing species determination and enumeration can provide critical information about—for instance—harmful algae blooms (HABs) or spreading of invasive species. A crucial step in current methods is the use of sedimentation. This provides the enrichment needed to achieve statistical counts of sometimes rare species within reasonable timeframes, but it comes with the drawback of aggregating the sample. This is a real challenge for computer-aided identification as particle aggregates can often be erroneously classified. In this paper, we propose an alternative method based on flow-through imaging aided by acoustic-focussing, as this provides better input-data for automated counting-methods while simultaneously removing the need for manual sample preparation. We demonstrate that by acoustically focussing microalgae and other particulates in a fast-flowing water sample, it is possible to analyse up to 8 mL sample per minute with sufficient image quality to discriminate the invasive species *Ostreopsis ovata* from other particulates in samples taken directly from the Mediterranean. We also showcase the ability to achieve sharp images in flow-through at magnifications up to × 50.

Keywords Microfluidics · Acoustics · Acoustofluidics · *Ostreopsis ovata* · High-throughput screening · Imaging cytometry · Environmental monitoring

Introduction

Microalgae are unicellular organisms found abundantly in both fresh and saline water bodies. There is a large variety of species and some are of major ecologic importance. As microalgae feature strong adaptability to the environment and quickly react to most environmental stressors in a predictable fashion, they provide measurable signals of a changing environment. Extensive and uncontrolled growth of microalgae may result in threatening effects in marine and freshwater ecology, impacting for instance fishery resources or quality of life. In particular, harmful algae blooms (HABs) are of special relevance, as they can generate toxins that affect human health and strongly impact the economy and exploitation of water resources.

Despite the crucial importance of monitoring microalgae, a method for rapid and precise recognition and classification is currently not available at an affordable price. Current methods to perform real-time identification of microalgae are either based on molecular biology or microscopy (Anderson et al. 2012). The former uses identification of specific genetic sequences and provides very high specificity and sensitivity. DNA-based assays have demonstrated to be robust and reliable and the adoption of barcoding strategies can provide a certain degree of generality (Hering et al. 2018). Nevertheless, molecular methods typically require expensive devices, the use of reagents and potentially challenging sample preparation. For these reasons, morphological assessment through microscopy is still the most widely used approach for microalgae classification and often the only certified method at regulatory level (Anderson et al. 2001).

The current standard in using digital microscopy to monitor phytoplankton requires a number of steps: sample collection, fixation (to avoid sample degradation), sedimentation, microscopy inspection and classification. The adoption of standardised protocols and procedures has strongly enhanced the repeatability of such measurements (Jauzein et al. 2018)

✉ Björn Hammarström
bham@kth.se

1 School of Engineering, University of Southampton, Southampton, UK

2 Biomedical and X-ray Physics, KTH Royal Institute of Technology, Stockholm, Sweden

3 Institute of Biophysics of the Italian National Research Council, Genoa, Italy

and the use of automated imaging platforms can ease and speed up image acquisition (Sbrana et al. 2017). This enables automatic digitalisation of a complete sample located on the surface of a sedimentation chamber. The large quantity of data obtained by this procedure is used in dedicated software procedures to distinguish and classify the phytoplankton (Coltelli et al. 2014). The accuracy of such methods is increasing rapidly as advances in artificial intelligence can be readily applied to this problem (Zheng et al. 2017). The resulting methodology can achieve identification performance comparable to human experts or molecular identification (Vassalli et al. 2018).

In these techniques, the need for a sedimentation step imposes a crucial drawback, as this typically requires several hours, or even overnight, for completion and rules out the possibility to get real-time estimates of algae abundance (relevant in case of harmful algal blooms). To avoid the sedimentation step and thereby extend the applicability of automated phytoplankton recognition to real-time scenarios, the most promising strategy is to use in-flow identification. This was pioneered at the end of the last century (Sieracki et al. 1998) in a device where controlled water flow is directly imaged inside a fluidic channel. This method has also been translated to a commercial instrument (FlowCam, Fluid Imaging Inc., ME, USA) which is used to observe phytoplankton in laboratory environments. While many technological advancements in imaging flow cytometry have been made in recent years (Lai et al. 2016; Nitta et al. 2018), the high unit cost of the system has so far prevented large-scale adoption (Wong et al. 2017) for everyday monitoring tasks.

In the pursuit of cheaper and more readily available devices, microfluidics and Lab-on-a-Chip (LOC) platforms may offer new possibilities (Campana and Wlodkowic 2018), one such example is spectroscopic investigation inside a microfluidic channel (Hiramatsu et al. 2019). Nevertheless, the extension of this approach towards in-flow imaging and high-throughput sedimentation-free automated identification has still to be demonstrated.

The use of acoustic radiation forces to manipulate cells in microfluidic systems, or acoustofluidics, is well established (Bruus et al. 2011; Laurell and Lenshof 2014). Typically, standing wave patterns are created at MHz frequencies, creating time-averaged forces that relate to the acoustic field distribution (Bruus 2012). A well established and arguably one of the most simplistic arrangements is the half-wave resonator, which creates a focus along a central plane of a channel (Glynne-Jones et al. 2012). Half-wave arrangements have been used to, for instance, remove the need for sheet flows in both Coulter counters (Grenvall et al. 2014) and in commercial instruments such as the Attune (Thermofisher, MA, USA). Furthermore, the acoustic properties of several species of microalgae have been investigated (Hincapié Gómez et al. 2018). A recent paper (Olson et al. 2017) incorporated an

acoustic focussing stage into a FlowCytobot (McLane, MA, USA) instrument and demonstrated enhanced performance.

For flow-through imaging in LOC-devices, acoustic forces offer the ability to finely control the position of particulates in a flowing sample (Zmijan et al. 2015). In morphology-based phytoplankton studies, precise control of the position is required for high-resolution images which will provide a much greater level of detail to be used for the subsequent classification. Importantly, objectives with high numerical aperture will provide a much-improved image quality but inherently have a small depth of focus. To enhance the overall performance, we also highlight two other factors. Enrichment is highly valuable in order to achieve statistical count of rare species at low concentrations within reasonable timeframes. Proper sample handling is critical in order to avoid aggregation, clogging or sedimentation. In this context, sedimentation is especially challenging as it will introduce significant challenges for any automated classification algorithm when multiple particles are co-located in an aggregate.

In this paper, we present an open and low-cost system that allows high-throughput imaging of phytoplankton at relevant concentrations. The system is not interfaced with an expensive commercial instrument but based on a simple acoustic system and μs-flashes from a LED-circuit (Willert et al. 2010). We characterise the device performance in detail and find that a particular advantage of the system is that no hydrodynamic focussing is required. This leads to positional control and the ability to use optics with a high resolution.

Methods

An acoustofluidic flow cell

An acoustofluidic flow cell (Fig. 1a) was realised using low-cost rapid prototyping methods as previously presented (Zmijan et al. 2015). Briefly, a laser cutter was used to define a channel outline in adhesive transfer tape (3 layers of 468MP, 3M, USA). The transfer tape was bonded between two double-width microscope slides of thickness 1 mm. Fluidic access holes, 1 mm in diameter, were drilled using a diamond-coated drill bit. A $1 \times 2.5 \times 5$ mm lead zirconate titanate (PZT) piezoelectric transducer (PZ-26, Ferroperm, Kvistgaard, Denmark) was attached using low-viscosity epoxy (Epotek-301, Epoxy Technology, Inc., USA) directly underneath the channel. On the transducer, a wrap-around electrode, joining the top-surface to a separate electrode on the back side of the piezo, was created using conductive silver paint (SCP Silver Conductive Paint, Electrolube Ltd., UK).

The inner dimensions of the channel were 320 μm × 6 mm, allowing laminar flow conditions to be maintained at all the used flow rates. While the narrow height produced a parabolic
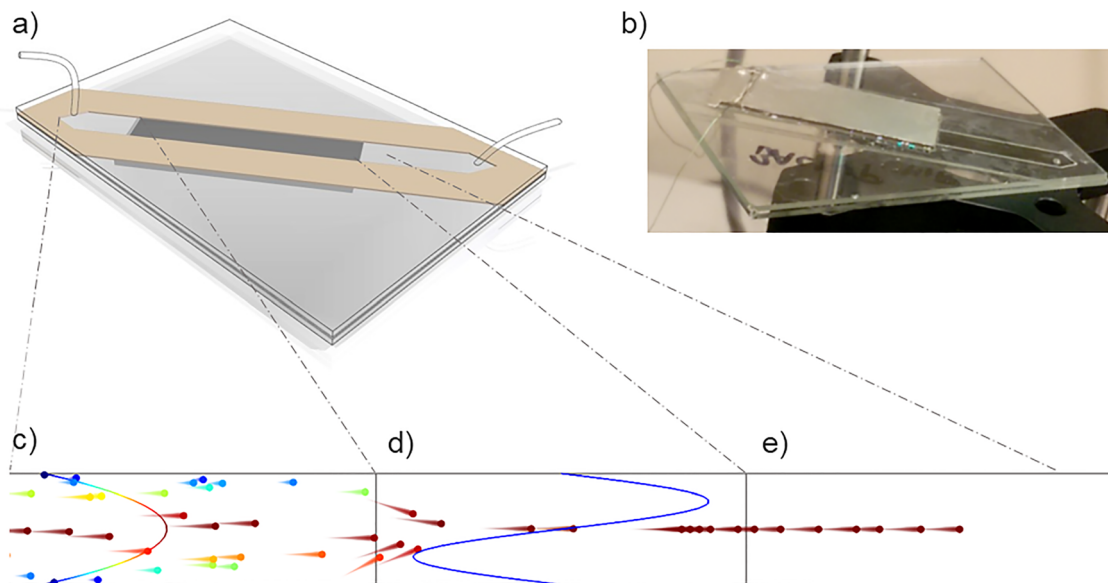
Fig. 1 The acoustofluidic flow cell **a**–**b** enables high-throughput imaging of microalgae by pre-aligning them to the focus plane of a microscope. A particle tracing (as described in the "Methods" section) illustrates how the particle velocities which are initially randomly distributed **c**, become uniform in the region above the transducer due to the acoustic-force focusing the particles to the same height **d**. Downstream from the transducer **e**, the particles are available for trans-illumination microscopy using pulsed LED illumination. The parabolic flow is shown in **c** and colour-coded such that the high-velocity particles are shown in red and low-velocity particles are blue. The length and direction of the comet-tail on the particles also show direction and magnitude of the velocity

flow profile in the height direction, designing the channel to be much wider than the imaging region meant that in this area, the flow profile was essentially uniform across the imaged width.

Modelling using a transfer impedance approach (Glynne-Jones et al. 2012) established that this arrangement of layer thicknesses would support an effectively coupled half-wave resonance, which was found experimentally at 2.10 MHz. The half-wave resonance was probed using beads and found to exert forces towards the central plane of the channel as expected. Thus, the resonator effectively focussed particles towards the imaging plane of the camera system.

A 2-dimensional COMSOL Multiphysics particle tracing simulation was used to model particle trajectories when subjected to an acoustic force in the transducer region (Fig. 1b, c). In this simulation, a mean inflow corresponding to 10 mL min^{-1} and sinusoidal acoustic force profile with sufficiently high amplitude were used as inputs to visualise the process. This showed that under such conditions, particles could be expected to move from a random distribution along the height into the centre of the channel and achieve the same velocity once they were centred.

A stroboscopic imaging strategy

While this work points towards a low-cost system, for simplicity and rigorous evaluation, the flow cell was mounted in a lab microscope (IX71, Olympus, Japan) imaging in a region downstream from the opaque transducer so that properly adjusted Koehler trans-illumination could be used. We evaluated objectives with magnifications 10, 20 and 50 times and in order to probe the upper limits of sample throughput, we used a scientific camera (ORCA Flash-4, Hamamatsu, Japan) that was run at full resolution (2048 × 2048). The used camera sensor had an effective area (EA) of 13.3120 × 13.3120 mm such that the field-of-view (FOV) became 4.2096 × 4.2096 mm, 2.9767 × 2.9767 mm and 1.8826 × 1.8826 mm for the respective magnifications. The FOV was set at 5 mm from the edge of the transducer, near enough to prevent sedimentation from being significant.

During high-throughput imaging, microalgae and other particles reach high velocities. As the camera had a maximum framerate of 90 fps, the high particle velocity generated motion blur with conventional illumination. To enable sharp images, a LED-based stroboscopic illumination capable of producing μs-pulses was used. A 3D-printed manifold was used to replace the halogen-bulb in the microscope bright field light-source with a high-brightness LED (LZ1-00G102, LED Engin, CA, USA). A frame-synchronised trigger signal from the camera was received by a microcontroller circuit (Arduino Uno, Arduino) programmed to send out one or several 5–10 μs long pulses within the 11 ms frame exposure time. An electronic circuit, triggered by the pulses, delivered high-current pulses to the LED. The circuit was fabricated using the capacitor discharge arrangement described by Willert et al. (2010).

While cameras with sufficiently low exposure times (or fast shutters) in order to remove the motion blur exist on the

market, a LED-based approach presents advantages in terms of cost and flexibility. Firstly, the approach is compatible with cameras lacking these features, so if limited funds are available a low-cost system can be realised by making light sensitivity and resolution a priority instead. Secondly, different excitation sequences (pulse-trains) has the potential to be used for coded excitation in order to enhance image quality (Gorthi et al. 2013) or provide additional information such as particle velocity. Furthermore, the narrow bandwidth illumination of the LED could be selected to be close to absorption peaks of for instance chlorophyll-*a* in order to provide enhanced contrast or absorption data if multiple LEDs were used. It is important to note that a LED used in pulsed mode is able to sustain higher currents, with an increase the brightness, compared to continuous mode (Willert et al. 2010).

Microalgae samples

Euglena gracilis is a commonly used model organism and was used to optimise operating parameters. The *E. gracilis* was cultured in freshwater media at room temperature using a timer-controlled lamp. When imaging, live *E. gracilis* samples from culture was used directly or diluted in water.

Samples labelled B3, B4 and B5 were collected on the Tirrenic coast by the Sardinia Regional Environmental Agency (ARPA Sardegna) in the framework of an institutional inter-calibration activity (Borrello et al. 2017) coordinated by the Italian Institute for Environmental Protection and Research (ISPRA). In accordance with standardised protocol, these samples were preserved in acetic-Lugol solution and screened for the toxic and invasive species *Ostreopsis ovata* both by manual counting by a taxonomist and by an automated imaging system utilising sedimentation (OvMeter; Vassalli et al. 2018). This enumeration was used as reference to evaluate classification and counting of *O. ovata* in our sedimentation-free system.

Results

Acoustic focussing

It was possible to acoustically focus live *E. gracilis* samples at flow rates exceeding 10 mL min^{-1}. At this flow-rate, the *Euglena* were still in sharp focus and the limiting factor for throughput was the imaging speed of the camera (as increase flow rates would result in some organisms not being imaged).

In order to assess the focussing performance in the height direction, the relationship between flow velocity and height in the device was used to infer focussed height from particle velocity (as determined by the parabolic flow distribution and laminar regime). Pulsed illumination was used to quantify the focussing performance at 10 mL min^{-1}. Programming the

microprocessor to generate two flashes (10 µs) separated by a fixed interval (700 µs) produced two identical images of the same microalga in each frame. An area around each object was selected by segmentation and cross-correlated with the original image. In this way, the displacement of each object could be automatically identified. It was found that progressively increasing the amplitude produced a tighter velocity distribution and that a Gaussian-like distribution with a centre close to 135 mm s^{-1} was obtained at sufficient voltage (Fig. 2). It was also found that the acoustic focussing could be confirmed by evaluating the sharpness of imaged objects, but the former method also provides information on the velocity of the particles. When imaging live *Euglena*, it was found advantageous to maintain a high flow rate (> 1 mL min^{-1}) to
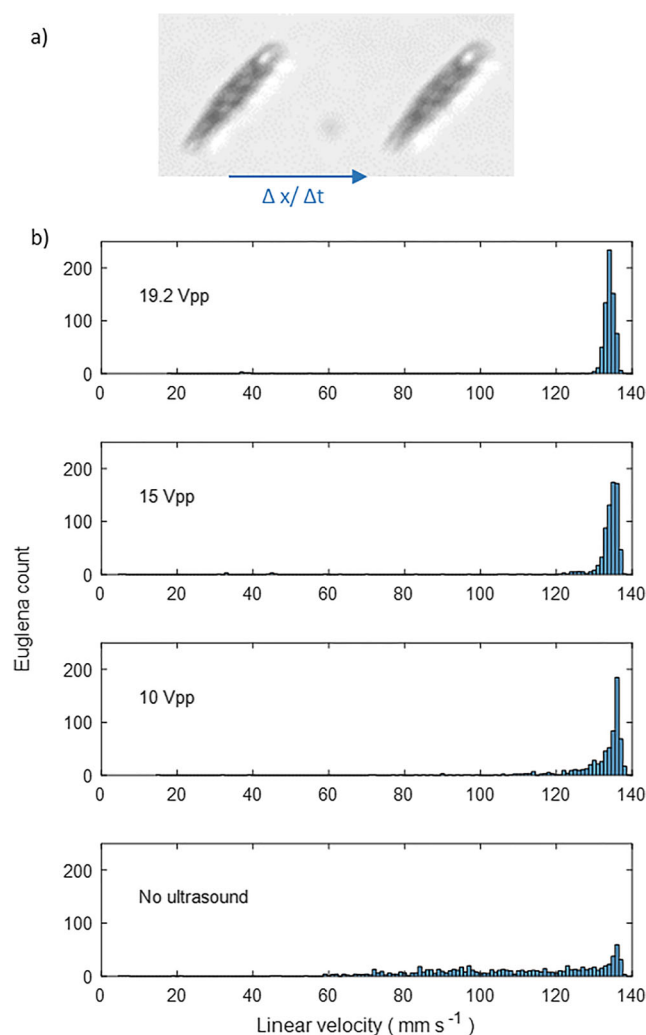
Fig. 2 Setting the LED to make two consecutive flashes during a single exposure allowed quantitative assessment of focusing for *Euglena gracilis* **a** at 10 mL min^{-1}. By this method, the same microalga is imaged twice and can be used to assess the velocity by using the displacement and the time interval between the flashes. At high amplitudes, the cells have a narrow velocity distribution and when gradually decreasing the amplitude to zero the distribution gets smeared

prevent the alga from swimming out of focus between the acoustic focussing and imaging regions.

At the highest actuation voltage, the distribution was 138.8 ± 1.3 mm s^{-1}. Using a parabolic flow profile approximation, this corresponds to ± 4.2 μm variation in particle centre position.

In-flow image quality

The pulsed illumination system produces images without motion blur at magnifications $\times 10$, $\times 20$ and $\times 50$ for relevant flow rates. Figure 3 shows close-up zooms of *O. ovata* imaged at flow rates 8 mL min^{-1} for $\times 10$ and $\times 20$ and 2 mL min^{-1} for $\times 50$ (see the "Discussion" section for why these flow rates were used). Although the *E. gracilis* samples were found to focus well at 10 mL min^{-1}, when using the seawater samples containing *O. ovata*, it was found that reducing the flow rate to 8 mL min^{-1} was more robust since larger objects (e.g. plastics or shrimps) would sometimes disturb the flow. For the selected flows and magnifications, Fig. 3 shows that all three magnifications can be used and neither motion blur, axial focus, nor light intensity is a limitation.

Automated counting of *Ostreopsis ovata*

Our device was integrated with a simplistic form of automatic counting (gating). More sophisticated algorithms which include recognition could be implemented, but our aim in this paper is to demonstrate that the acoustofluidic method, which can produce high-quality image sequences rapidly from raw samples with minimal sample preparation, is a viable platform for counting and identification. We focused on *O. ovata*, a harmful species featuring large blooms during summertime and whose concentration is measured by marine agencies in the context of specific national monitoring regulations (Vassalli et al. 2018). The concentration of *O. ovata* in the

seawater was estimated by collecting $\times 10$ magnification snapshots and implementing an image filter algorithm in the MATLAB Imaging Toolbox. The images were segmented and subsequently thresholds were set on particle area, perimeter, aspect-ratio and mean-intensity.

This approach is essentially a form of gating, as is commonly used in flow cytometry. After segmentation, a wide array of parameters are conceivable but the above four were used as they gave rise to visible clustering of the data. The range limits were subsequently set to isolate the observed clusters as shown by red boxes in Fig. 4a and b. This approach was then verified by checking that the assigned classification matched the visual assessment of this particular species for approximately 10% of the images in each set, Fig. 4c.

In order to ensure a homogenous suspension with minimal aggregation, a particular procedure was adopted when loading the samples. The 10 mL samples were loaded into a syringe from a conical vial by first aspirating 70% of the sample and then flushing it back out. This was found to be an effective and reproducible way of re-suspending the sample prior to loading it into the syringe. A valve was then used to infuse the sample into the flow cell and since the complete 10-mL water sample could be processed in just over 1 min no significant sedimentation could be observed during the processing itself.

During perfusion of the sample, a fraction of the available time was used for imaging as it was sufficient for the analysis and provided a manageable amount of image data (300 frames, corresponding to 3.3 s). Resulting counts for the three samples (B3, B4 and B5) are shown in Fig. 4d.

Compared to the previously established results on these same samples, quantitative comparison of the counts obtained through the acoustic method with gating compares well with both the taxonomist count and the sedimentation-based algorithmic classification (henceforth called OvMeter). At higher concentrations, the difficulties with sedimentation-based
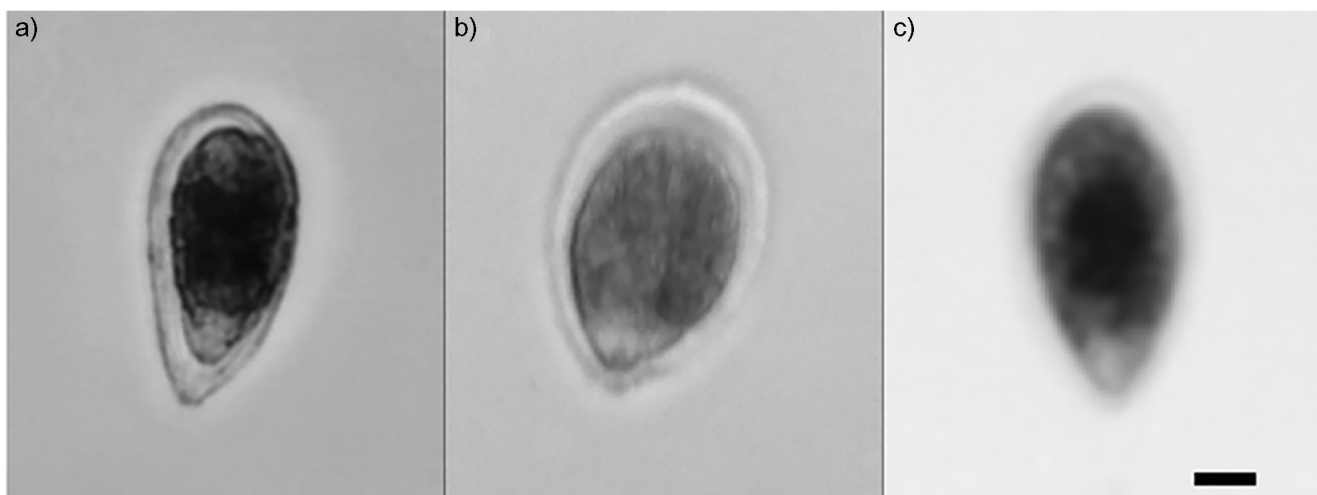

Fig. 3 Comparison of the level of detail obtained at $\times 50$, $\times 20$ and $\times 10$ magnification while imaging acoustically focussed *Ostreopsis ovata* at a flow rate of 8 mL min^{-1} for $\times 20$ and $\times 10$ and 2 mL min^{-1} for $\times 50$. The images are scaled such that the 10 μm scale bar applies to all three images
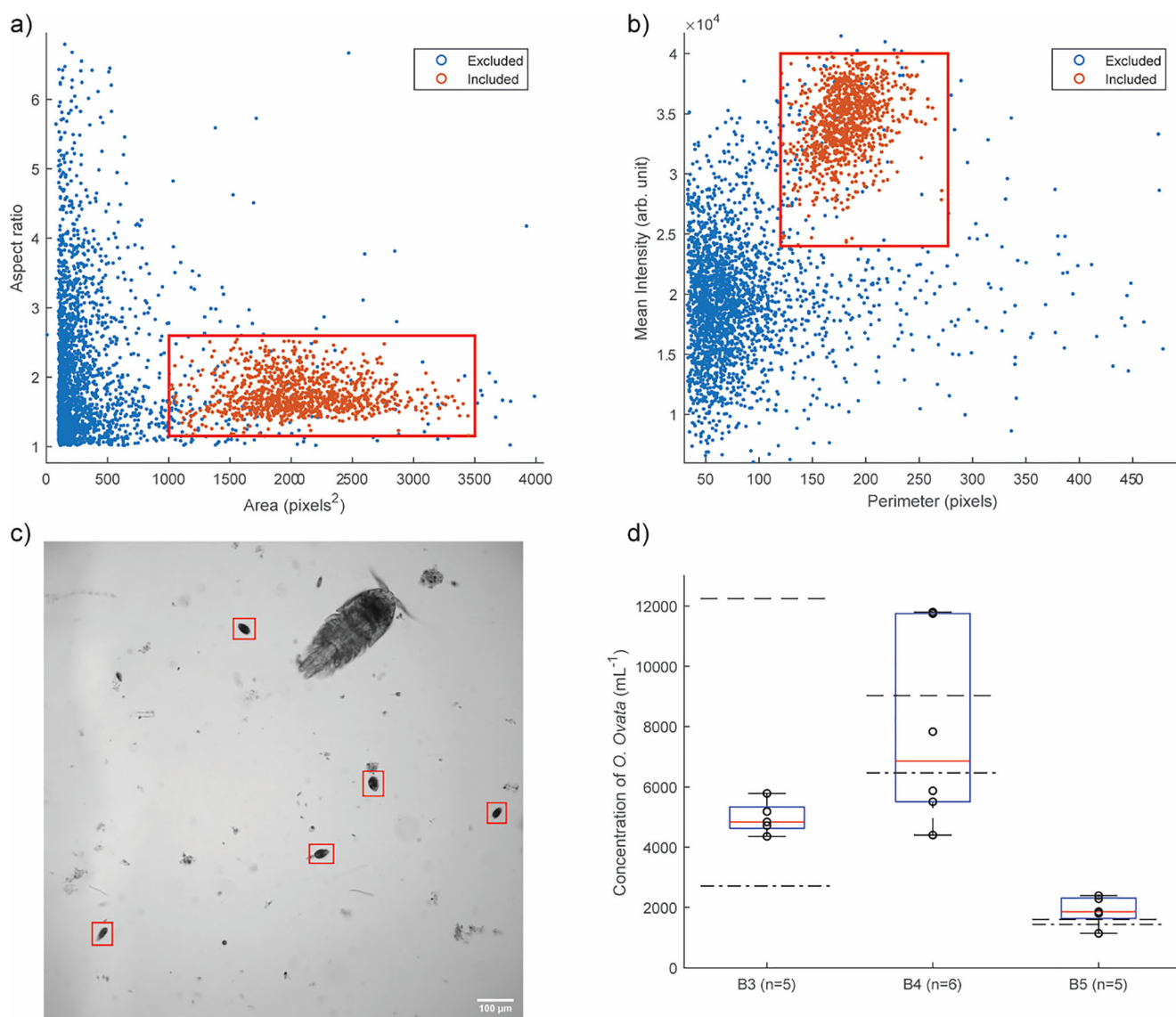
Fig. 4 Results for *Ostreopsis ovata* in water samples from the Mediterranean. The dots in figure **a–b** show each segmented object in the images and if it falls inside the criteria set for area, aspect ratio, perimeter and mean intensity, it is coloured orange, else it is coloured blue. The first gate **a** is set on the parameters aspect ratio (height to width) and area, where a clear subpopulation appears. The second gate **b** is set on intensity and perimeter (or circumference), also here a subpopulation appears. If an object falls within these limits, it is regarded as being an *O. ovata* and is also highlighted with a red square in the original photo **c**. In the photo, large amounts of debris (such as plastics) and other species are also visible but not counted. *O. ovata* concentration was quantified for three samples **c**, shown in box-and-whiskers plots (the centre-line is the median and the edges of the box indicate the 25th and 75th percentile) with the individual data points as an overlay. Here, the same sample was processed several times ($n = 5$, 6 and 5) and each time, 300 frames were analysed. For comparison, the concentrations for these samples measured by manual counting are indicated by a dashed line, and the results of an alternative automated counting method based on algorithmic classification are indicated by a dash-dot line

methods are exaggerated as the chance of overlapping cells due to higher aggregation. This is obvious in the first sample (B3), which has the highest algae concentration, and proved to be difficult to automatically count with standard methods as appears from the huge difference between the taxonomist count of 12,240 mL^{-1} and the OvMeter result of 2714 mL^{-1}. Here, the acoustic method with gating results in 4977 mL^{-1} which is closer to the manual count. The above is also true for sample B4 where the acoustic method produced a value closer to the taxonomist (9027 mL^{-1}) than the OvMeter (6462 mL^{-1}). In sample B5, an agreement between all three methods (Taxonomist 1600 mL^{-1} and OvMeter 1434 mL^{-1}) was found.

Discussion

Successful operation at high volumetric flow rates is a critical requirement when analysing water samples without prior

enrichment by filtration or sedimentation. We have demonstrated that acoustic focussing can effectively bring phytoplankton within the depth of field of a ×50 objective at high flow rates. We have quantified the variations in particle velocities and used these to gauge the variations in z-position of the particles (Fig. 2). A likely source of variations in the velocities is the distribution in size and shapes of the organisms themselves. This is reasonable since larger organisms will span a wider range of flow velocities and thus experience a lower mean flow velocity. This effect may also be exaggerated by the fact that the acoustic focus plane is not identical with the centre of the channel. Therefore, the flow profile is not necessarily symmetric around the particle centre producing further size-dependent variations in mean flow velocity. This means that the small positional variation can most likely be attributed to variations in size and orientation of the microalgae. Furthermore, prior investigations with an equivalent device (Zmijan et al. 2015) have shown it capable of an acoustic focussing accuracy better than 3 μm when applied to 10 μm polystyrene microbeads. Ultimately, the image quality (in particular at ×50 magnification) confirms that the accuracy of the acoustic focus is sufficient for the application.

The analytic flow rate can be defined as the actual volume of fluid imaged by the device. In this system, the analytic throughput is lower than the actual sample throughput as only a proportion of the flow is imaged. This proportion varies with the field of view of the microscope. The analytic flow rate is limited in the current system by the imaging rate of the camera, as above a certain flow rate the sample moves more than a field-of-view between frames. At all flow rates presented here, the acoustic focussing is sufficient to achieve good positional focussing of the phytoplankton to enable sharp images. Figure 5 shows how the analytic flow rate varies with flow rate for our system, transitioning between a linear region, limited by the flow-rate, to a plateau where further increases in flow rate do not increase analytic flow rate due to the camera frame rate limit being reached. At ×10 magnification, for example, maximum analytic throughput is 2.04 mL min^{-1} (for 90 fps). For magnifications ×20 and ×50, the analytic throughput is limited by the camera for our system. Therefore, we anticipate that if faster cameras become available, they may primarily increase performance at these magnifications.

In situations where the target microalgae are in low concentrations (occurring as rare events), the analytic throughput can be the limiting factor for detection within reasonable timescales. It is thus encouraging to find that the acoustic focussing is effective even at high flow rates. In rare event scenarios, alternative imaging strategies might also be employed such as using multiple pulses of illumination during a single camera frame in order to capture information from multiple volumes of sample or using a photomultiplier based detector to trigger imaging pulses.
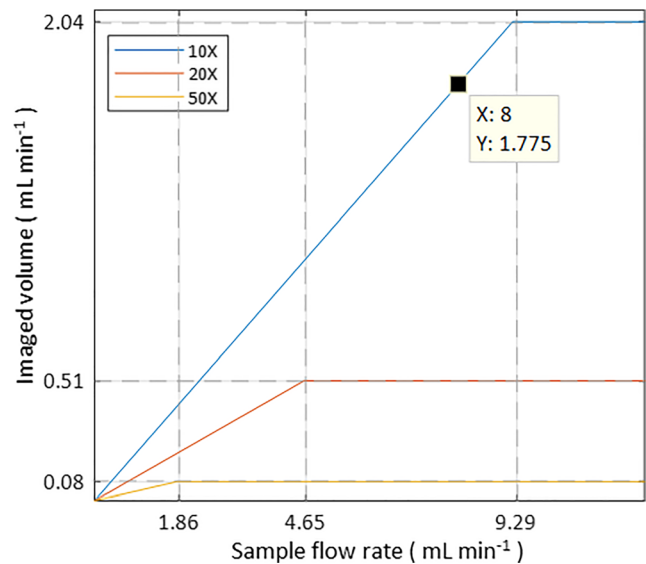

Fig. 5 The analytic throughput or imaged sample volume rate is linearly related to the sample flow rate until the data transfer rate of the camera becomes the limit. Both the slope of the linear relationship and point at which the graph levels off depends on the magnification. Significant improvements in speed can be obtained by not using higher magnification than necessary. The acoustic focussing provides effective positioning at all points up to 10 mL min^{-1} for our pure *Euglena gracilis* test samples. For the marine samples containing *Ostreopsis ovata*, a sample flow rate of 8 mL min^{-1} could be reached of which 1.8 mL min^{-1} (the analytical throughput) was imaged.

It is also important to realise that the acoustic focussing is a form of pre-enrichment: Initially, the sample is distributed over the full height of the chamber (320 μm) and becomes concentrated into the central region where it becomes accessible to the depth of field of the objective. This is in contrast to hydrodynamic focussing, where the entire, diluted sample volume has to be imaged. In this way, the analysis process can be streamlined, removing the need for pre-enrichment steps, allowing samples to be used immediately after capture. We also note that the acoustic focussing reduces fluidic complexity in the system, leading to lower costs and greater reliability.

The system presented here has shown to be a viable option for automated imaging on a coverslip or manual investigation by a taxonomist, as demonstrated by successfully analysing real marine samples. Here, we found that a slightly reduced flow rate of 8 mL min^{-1} (instead of the maximum of 10 mL min^{-1}) was advantageous as the large variety of particulates, such as large pieces of plastic or small shrimps, would temporarily interfere with the focus when passing at maximum speed. We found that the *O. ovata* were well dispersed from each other and that by keeping the sample well suspended before infusion the amount of aggregates could be kept to a minimum.

As image analysis is not the primary focus in this paper, we use a rather simplistic gating method to count the *O. ovata*. This was also done at low magnification to showcase the imaging and throughput strengths of the system and proved effective for these samples. Nevertheless, the acoustic focusing device also allows the acquisition of high-resolution images, required to spot fine differences between similar species, as in the case of *O. ovata* with respect to *Ostreopsis fattorussoi* (Vassalli et al. 2018). This crucial feature opens up for future application of advanced machine learning algorithms, to further enhance the overall performance of the identification process. In contrast to more conventional approaches, imaging cytometry does not require a sedimentation step, thus an instrument based on this technology should be capable of producing rapid results with minimal user intervention and sample handling.

As such, the demonstrated ability to image at high magnifications shows that there is a tremendous potential for successful application in a diverse range of phytoplankton-monitoring tasks. In conclusion, the acoustofluidic system presented here paves the road for the future developments of rapid, cheap and high-resolution imaging platforms for automatic real-time marine phytoplankton identification in a variety of samples.

Data availability Data used to produce the figures in this paper is openly available from the University of Southampton repository at https://doi.org/10.5258/SOTON/D1074.

References

Anderson DM, Andersen P, Bricelj VM, et al (2001) Monitoring and management strategies for harmful algal blooms in coastal waters. Asia Pacific Economic Program, Singapore, Intergov Oceanogr Comm Tech Ser No 59 APEC #201-MR-011 pp 1–268

Anderson DM, Cembella AD, Hallegraeff GM (2012) Progress in understanding harmful algal blooms: paradigm shifts and new technologies for research, monitoring, and management. Annu Rev Mar Sci 4:143–176

Borrello P, Spada E, Asnaghi V, Chiantori M, Vassalli M, Sbrana F, Ottaviani E, Giussani V (2017) Valutazione del sistema automatico di identificazione e conteggio di cellule di *Ostreopsis ovata*. ISPRA Rapp 263:1–46

Bruus H (2012) Acoustofluidics 2: perturbation theory and ultrasound resonance modes. Lab Chip 12:20–28

Bruus H, Dual J, Hawkes J, Hill M, Laurell T, Nilsson J, Radel S, Sadhal S, Wiklund M (2011) Forthcoming lab on a chip tutorial series on acoustofluidics: acoustofluidics—exploiting ultrasonic standing wave forces and acoustic streaming in microfluidic systems for cell and particle manipulation. Lab Chip 11:3579–3580

Campana O, Wlodkowic D (2018) The undiscovered country: ecotoxicology meets microfluidics. Sensors Actuators B 257:692–704

Coltelli P, Barsanti L, Evangelista V, Frassanito AM, Gualtieri P (2014) Water monitoring: automated and real time identification and classification of algae using digital microscopy. Environ Sci Process Impacts 16:2656–2665

Glynne-Jones P, Boltryk RJ, Hill M (2012) Acoustofluidics 9: modelling and applications of planar resonant devices for acoustic particle manipulation. Lab Chip 12:1417–1426

Gorthi SS, Schaak D, Schonbrun E (2013) Fluorescence imaging of flowing cells using a temporally coded excitation. Opt Express 21:5164–5170

Grenvall C, Antfolk C, Bisgaard CZ, Laurell T (2014) Two-dimensional acoustic particle focusing enables sheathless chip coulter counter with planar electrode configuration. Lab Chip 14:4629–4637

Hering D, Borja A, Jones JI, Pont D, Boets P, Bouchez A, Bruce K, Drakare S, Hänfling B, Kahlert M, Leese F, Meissner K, Mergen P, Reyjol Y, Segurado P, Vogler A, Kelly M (2018) Implementation options for DNA-based identification into ecological status assessment under the European Water Framework Directive. Water Res 138:192–205

Hincapié Gómez E, Tryner J, Aligata AJ, Quinn JC, Marchese AJ (2018) Measurement of acoustic properties of microalgae and implications for the performance of ultrasonic harvesting systems. Algal Res 31:77–86

Hiramatsu K, Ideguchi T, Yonamine Y, Lee S, Luo Y, Hashimoto K, Ito T, Hase M, Park JW, Kasai Y, Sakuma S, Hayakawa T, Arai F, Hoshino Y, Goda K (2019) High-throughput label-free molecular fingerprinting flow cytometry. Sci Adv 5:eaau0241

Jauzein C, Açaf L, Accoroni S, Asnaghi V, Fricke A, Hachani MA, Saab MA, Chiantore M, Mangialajo L, Totti C, Zaghmouri I, Lemee R (2018) Optimization of sampling, cell collection and counting for the monitoring of benthic harmful algal blooms: application to *Ostreopsis* spp. blooms in the Mediterranean Sea. Ecol Indic 91:116–127

Lai QT, Lee KC, Tang AH, Wong KK, So HK, Tsia KK (2016) High-throughput time-stretch imaging flow cytometry for multi-class classification of phytoplankton. Opt Express 24:28170–28184

Laurell T, Lenshof A (eds) (2014) Microscale Acoustofluidics. Royal Society of Chemistry, Cambridge

Nitta N, Sugimura T, Isozaki A, Mikami H, Hiraki K, Sakuma S, Iino T, Arai F, Endo T, Fujiwaki Y, Fukuzawa H, Hase M, Hayakawa T, Hiramatsu K, Hoshino Y, Inaba M, Ito T, Karakawa H, Kasai Y, Koizumi K, Lee SW, Lei C, Li M, Maeno T, Matsusaka S, Murakami D, Nakagawa A, Oguchi Y, Oikawa M, Ota T, Shiba K, Shintaku H, Shirasaki Y, Suga K, Suzuki Y, Suzuki N, Tanaka Y, Tezuka H, Toyokawa C, Yalikun Y, Yamada M, Yamagishi M, Yamano T, Yasumoto A, Yatomi Y, Yazawa M, di Carlo D, Hosokawa Y, Uemura S, Ozeki Y, Goda K (2018) Intelligent image-activated cell sorting. Cell 175:266–276

Olson RJ, Shalapyonok A, Kalb DJ, Graves SW, Sosik HM (2017) Imaging FlowCytobot modified for high throughput by in-line acoustic focusing of sample particles. Limnol Oceanogr Meth 15:867–874

Sbrana F, Landini E, Gjeci N, Viti F, Ottviani E, Vassalli M (2017) OvMeter: an automated 3D-integrated opto-electronic system for

Ostreopsis cf. *ovata* bloom monitoring. J Appl Phycol 29:1363–1375

Sieracki C, Sieracki M, Yentsch C (1998) An imaging-in-flow system for automated analysis of marine microplankton. Mar Ecol Prog Ser 168:285–296

Vassalli M, Penna A, Sbrana F, Casabianca S, Gjeci N, Capellacci S, Asnaghi V, Ottaviani E, Giussani V, Pugliese L, Jauzein C, Lemée R, Hachani MA, Turki S, Açaf L, Saab MAA, Fricke A, Mangialajo L, Bertolotto R, Totti C, Accoroni S, Berdalet E, Vila M, Chiantore M (2018) Intercalibration of counting methods for *Ostreopsis* spp. blooms in the Mediterranean Sea. Ecol Indic 85:1092–1100

Willert C, Stasicki B, Klinner J, Moessner S (2010) Pulsed operation of high-power light emitting diodes for imaging flow velocimetry. Meas Sci Technol 21:075402. https://doi.org/10.1088/0957-0233/21/7/075402

Wong E, Sastri AR, Lin F-S, Hsieh C (2017) Modified FlowCAM procedure for quantifying size distribution of zooplankton with sample recycling capacity. PLoS One 12:e0175235. https://doi.org/10.1371/journal.pone.0175235

Zheng H, Wang R, Yu Z, Wang N, Zheng B (2017) Automatic plankton image classification combining multiple view features via multiple kernel learning. BMC Bioinformatics 18:570

Zmijan R, Jonnalagadda US, Carugo D, Kochi Y, Lemm E, Packham G, Hill M, Glynne-Jones P (2015) High throughput imaging cytometer with acoustic focussing. RSC Adv 5:83206–83216